4-1-2002

Clonal Fitness of Attached Bacteria Predicted by Analog Modeling

J. L.S. Murray

Peter Jumars
University of Maine - Main, jumars@maine.edu

Clonal Fitness of Attached Bacteria Predicted by Analog Modeling

J. L. S. MURRAY AND PETER A. JUMARS

Microbial ecology is undergoing a revolution of phenomenological discoveries and methodological advances that bring resolution down toward the level of the individual and highlight the role of chemical exchanges in bacterial communities. Recent work shows that inter- and intraspecific chemical signaling, leading to coordinated, density-dependent behavior (termed *quorum sensing*) (Fuqua et al. 1994), is commonplace among bacterial species (Fuqua et al. 1996, Kaiser and Losick 1997) and is relevant in natural habitats (McLean et al. 1997, Bachofen and Schenk 1998). Density-dependent phenomena, first identified in bioluminescence (Wilson and Hastings 1998), where the induced behavior is visible, have since been implicated in general foraging and defensive behaviors such as production of extracellular enzymes and antibiotics (Givskov et al. 1997, Chernin et al. 1998, Srinivasan et al. 1998).

An additional development is the recognition of the tremendous importance of surface-attached bacteria in nature (Costerton 1995). Increased acquisition of nutrients has been proposed as one explanation for attachment (Ben-Ari 1999). Surfaces are also habitats for microbial consortia, or groups of bacterial species whose interdependent metabolic reactions are required for the decomposition of certain complex substrates (Wolfaardt et al. 1994, Paerl and Pinckney 1996).

Improvements in molecular techniques for identifying taxa, phylogenetic relationships, and differential genotypic and phenotypic expression are accelerating (Pace 1997, Tunlid 1999). It is arguable that measurement capability has surpassed predictive expertise, particularly at the clonal level. Other authors have hypothesized that evolutionary processes operating at multiple taxonomic levels result in widespread cooperative behavior in bacteria, as exemplified by quorum sensing (Caldwell et al. 1997). Coevolution has been proposed to explain the close associations among consortial bacteria (Caldwell et al. 1997). In contrast to the progress being made in empirical microbial ecology, few theoretical treatments of these topics exist (Brookfield 1998).

USING A PHYSICALLY IMPLEMENTED ELECTRICAL ANALOG FOR NUTRIENT TRANSPORT, WE PREDICT THAT MAXIMAL FITNESS OF A CLONAL POPULATION OF ATTACHED BACTERIA MAY OCCUR WHEN THE POPULATION COVERS ONLY A SMALL FRACTION OF THE SURFACE

An exciting result of the rapid progress in microbial ecology is that methodologies and incentives now exist to treat bacteria like larger (i.e., easier to visualize) organisms, gaining from the application of existing general ecological theory to microbial problems. General ecology, on the other hand, is poised to benefit from applying such theory to microbial systems. Bacteria can be modeled almost perfectly in terms of morphologies, motilities, and growth, and they can be tested experimentally with billions of organisms and over many generations.

J. L. S. Murray (previously published as J. L. Schmidt) (schmidt@nceas.ucsb.edu) is a postdoctoral researcher at the National Center for Ecological Analysis and Synthesis at the University of California, Santa Barbara, CA 93101. Her research interests include the microbial ecology of marine sediments, including chemical communication and foraging strategies of bacteria. Peter A. Jumars (jumars@maine.edu) is a professor in the School of Marine Science at the University of Maine, Walpole, ME 04753. His research focuses on identifying and quantifying important mechanisms by which marine organisms interact with their physical and chemical environments.

One major difficulty is predicting performance of bacterial individuals, a key step in gaining understanding of most metazoans. For example, the relationships between individual foraging and local habitat are central to predicting the abundance of organisms in time and space. Additionally, quantifying the relationships between fitness and genetic relatedness is essential for understanding the evolution of cooperation (Dugatkin 1997). For bacteria, which are 0.2–2.0 μm in diameter and are often studied in samples of 10^5–10^9 organisms, these relationships have been difficult to elucidate. Theoretical treatments have thus far been limited to individual organisms and simple geometries (Koch and Wang 1982, Karp-Boss et al. 1996, Vetter et al. 1998, Dusenbery 1999, Ploug et al. 1999).

Here we quantify foraging by individual attached bacteria in those porous media where mass transport is dominated by diffusion. In particular, we focus on surficial marine sediments, where 99.9% of bacteria are attached to grain surfaces (Steward et al. 1996), forming sparse biofilms. Specifically, we quantify the cost of attachment in the currency of nutrient uptake and, given attachment, how uptake is influenced by sediment-grain microtopography. Additionally, we describe the impact of near-neighbor bacteria and initiate a foraging theory appropriate for clonal populations.

These issues require solutions to Fick's laws of diffusion for complicated geometries (see Box 1). Analytical solutions do not exist, and numerical estimates would require daunting boundary and grid specifications. Instead, we implement an electrical model, inspired by Berg's (1993) theoretical treatment, to quantify steady-state diffusive uptake by benthic bacteria.

Electrical analogs, based on mathematical equivalence among disparate systems, were used to solve transport problems before affordable digital computing became available (Karplus and Soroka 1959, Welty et al. 1984). Physically implemented electrical analogs had not been used previously to solve complex diffusion problems (except for a brief treatment in Segall et al. 1985, app. A), nor had they been used in ecological contexts. The method described here is accurate, economical, rapid, and flexible. It holds promise in contemporary education, as well, because a hands-on approach involving analogous thinking can greatly improve physical intuition, particularly regarding mass and energy transfer. Developing this understanding is especially important in biology, where interactions between organisms and their environments are often constrained physically. Furthermore, the analogy is well suited to interdisciplinary efforts emphasizing comprehension across multiple time and space scales (Rutherford and Ahlgren 1989, Moreno 1999).

Microbial foraging

Bacteria are osmotrophs (osmosis + nutrient): They acquire nutrients via the uptake of small dissolved molecules across the cell membrane. Thus, their foraging relies on the diffusion of nutrients to the cell surface. The thermal energy of a solute (or any) molecule is manifested as kinetic energy (the definition of which contains a velocity term), which propels the molecule. Molecules move rapidly and collide with myriad other (mostly solvent) molecules, which randomize the motion. The repeated starting and stopping, with random directional reorientation at each step, is diffusion on a microscopic scale. At a macroscopic scale, diffusion is the resulting exchange between parcels of differing solute concentrations. Both solute and solvent diffuse, but transport of solvent is described as osmosis. Macroscopic transport (Figure 1a) is the sum of the microscopic "random walks" of individual molecules (Berg 1993, p. 17). *Random walk* is a statistical term, first presented in 1905 by Karl Pearson (Kaye 1989), who is known by most biologists in reference to the Pearson correlation coefficient. A random walk is a process consisting of a sequence of discrete steps of fixed length; the randomness requires that the direction of each step is governed by chance independent of preceding steps (Weisstein 2000, "Random Walk"). Kaye (1989) presents a humorous and intuition-building approach to random walks that extends their application to many problems. Weisstein (2000) provides an excellent source of hyperlinked mathematical terms and definitions. From here forward, we use *diffusion* to describe the macroscopic process of solute transport.

Diffusive transport to a cell occurs when a concentration gradient surrounds the surface, and Fick's laws of diffusion can be used to calculate the diffusive transport (Box 1, Figure 2). In three dimensions, at steady state, diffusion follows Laplace's equation

$$\nabla^2 C[\text{mol m}^{-3}\,\text{s}^{-1}] = 0,$$

which says that the second spatial derivative of the concentration C[mol m^{-3}] is equal to 0 (symbols defined in Table 1). (See Box 1, note a, for a discussion of the Laplacian operator, ∇^2.) To predict diffusion to a microbe, Laplace's equation is solved for C under given boundary conditions. The diffusional flux J_{Diff} [mol m^{-2} s^{-1}], or transport rate per unit area, and the diffusional transport rate I_{Diff} [mol s^{-1}] are then calculated from the function C (Box 1, Figure 2).

Analytical and numerical solutions of Laplace's equation have modeled steady-state diffusion to single (Koch and Wang 1982, Berg 1993, Karp-Boss et al. 1996) and colonial (Ploug et al. 1999) planktonic osmotrophs of simple shapes. Their models, as well as those developed here, generally include two assumptions. First, they assume that the cell's uptake rate is equal to the diffusional transport I_{Diff} to the surface. This rate can be limited by either the rate of diffusional supply to the cell surface or the rate of transport across the cell membrane (Pasciak and Gavis 1974, Koch 1990, Karp-Boss et al. 1996). In either case, the rate corresponds to a constant substrate concentration at the cell surface. In the former case, the cell acts as a "perfect absorber" with the surface concentration equal to 0. The second assumption is that nutrient uptake is in steady state, implying that the time to reach steady-state absorption is generally much shorter than the time in which the environment changes. That is, concentration in the medium far from the cell also is assumed constant. The analog approach works by implementing the constancy in con-

centration in the medium and at the cell surface, thereby setting the gradient that drives diffusion.

Unfortunately, analytical solutions, pursued as above, do not exist for most real-world problems, particularly in porous media. Numerical approaches ("Laplace solvers") employ iteration on a specified grid in a problem space where boundary conditions are given by known functions. This approach is not feasible for complex grain surfaces and multiple cells, especially in three dimensions.

Another method of solution is to measure the process of interest in a physical model. When dimensional relationships are understood, length scales can be manipulated to make microscopic processes macroscopic. Diffusion of dye through gelatin (used to reduce the inevitable mixing by convection in aqueous solutions) can be used for simple situations (Berg 1993), but it is not a reasonable technique for complex problems because of difficulties in maintaining boundary conditions, measuring quantities, and waiting for steady state. The time t for a molecule to diffuse a distance x is

$$t[\mathrm{s}] \cong \frac{x^2}{2D},$$

where D [m^2 s^{-1}] is the molecular diffusion coefficient (Berg 1993). Magnifying a microbial problem 10^4–10^5 times in length (e.g., modeling a bacterium of 0.1 μm radius as an object of 1 mm to 1 cm radius) would require scaling by factors

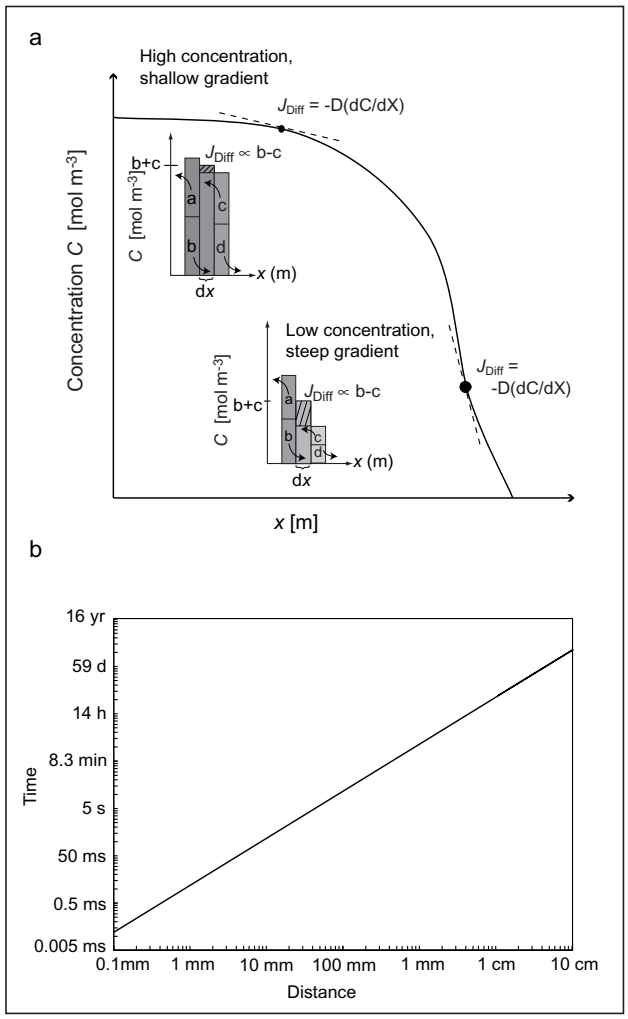

Figure 1. Basic diffusion phenomena. (a) Graphic and analytic illustration of Fick's first law of diffusion (one dimensional) and the dependence of mass transport on gradients, rather than magnitudes (see Box 2). Insets: In each parcel of length dx, over time step t, 50% of the solute molecules randomly walk to the left, and 50% randomly walk to the right. The replacement molecules come from the left (b) and right (c). Their sum equals the concentration C [mol m^{-3}], and their difference is proportional to the flux J_{Diff} [mol m^{-2} s^{-1}], shown by hatched regions. As dx → 0, the derivative form is appropriate, shown by the dashed lines. (b) Log–log plot of average time for molecular diffusion of sucrose in water at 25°C. Time to diffuse varying distances illustrates why scaled-up diffusion models of microscopic process would require a great deal of patience.

Table 1. Symbols used throughout the text and figures.

Symbol	Quantity	SI units[a] (alternate form[b])
A	Area	m^2
σ	Conductivity	A V^{-1} m^{-1}
C	Concentration	mol m^{-3}
D	Diffusion coefficient	m^2 s^{-1}
F	Fitness[c]	mol s^{-1}
I_{Diff}, I_{Elec}	Diffusive transport or electric current[a,d]	mol s^{-1} or A(Cs^{-1})
J_{Diff}, J_{Elec}	Solute flux or electrical flux (current density)	mol $m^{-2}s^{-1}$ or A m^{-2}(C $m^{-2}s^{-1}$)
M	Metabolic cost[a]	mol s^{-1}
N_B	Number of bacteria[e]	mol
r	Radial distance[f]	m
V	Electric potential[g]	V
x	Linear distance[h]	m

a. Units include ohms (Ω), amperes (A), coulombs (C), meters (m), seconds (s), volts (V), and kelvins (K).

b. Included for clarity in dimensional analyses of transport processes.

c. Subscripts "Ind" and "Clone" refer to processes for individual cells or clonal populations, respectively.

d. Subscript "Max" refers to the maximum transport measured or predicted. Subscripts "Free" and "Flat" describe transport to a bacterium that is freely suspended and to one that is abutted to a surface, respectively. Subscript "Full" refers to that obtained with a full monolayer of bacteria.

e. Subscript "Full" refers to the number required for a full monolayer.

f. Subscripts "In," "Out," "B," and "G" refer to inner, outer, bacterium, and grain, respectively.

g. Synonymous with "voltage" in older texts. Electric potential V always refers to a potential difference, either between the point of interest and a known reference point (ground) or between two points of interest. Because $(V_L - V_{Ground}) - (V_0 - V_{Ground}) = V_L - V_0$, the distinction is not usually pointed out.

h. Subscripts "L," "H," "S," and "F" refer to length, height, separation, and fluid (boundary), respectively.

of 10^8–10^{10} in time. A molecule of sugar in water at room temperature ($D \cong 1.0 \times 10^{-5}$ cm^2 s^{-1}) diffuses 1 μm in 5×10^{-6} seconds, but travels 1 cm in 14 hours, far too slow for practical experiments (Figure 1b).

Analogy and similitude

Many authors (Gebhart 1993, Cussler 1997) show that problems described by the diffusion equation are interchangeable with problems described by the heat conduction equation (known as Fourier's law),

$$\frac{\partial \nu}{\partial t} = \kappa \nabla^2 \nu,$$

with thermodynamic temperature ν [K] and thermal diffusivity κ[m^2 s^{-1}]. Thus, a solution of the heat equation (e.g., those found in Carslaw and Jaeger 1959) can be applied directly to an analogous diffusion problem by replacing ν with C [mol m^{-3}] and κ with $-D$ [m^2 s^{-1}]. At steady state, heat conduction is governed by Laplace's equation for temperature, $\nabla^2 \nu = 0$. Diffusion of mass and heat both result from random motions of molecules; diffusion changes the molecular distribution, and heat conduction changes the thermal energy distribution. The terminology is similar, and boundary conditions compare easily (e.g., constant solute concentration versus constant temperature). Both transport rates depend not on absolute magnitudes but on gradients (of concentration or temperature).

We stress here that every physical process that obeys Laplace's equation is analogous to, or has similitude to, diffusion (Table 2). Vaux (1961), Johnson (1999), and Narasimhan (1999) developed in-depth analogies among transport processes. These analogies are based on linear responses to spatial gradients, generally resulting from random walks or random walks with drift (due to an applied force). They also rely on steady state. Biologists can readily apply "analogous thinking" (Johnson 1999) to conceptualize and quantify physical processes, providing immediate benefits in physical intuition from more familiar systems.

Berg and Purcell (1977) and Berg (1993) presented a theoretical electrical analog, based on Laplace's equation for electrostatic potential in charge-free space, to solve challenging diffusion problems. Berg (1993) presented a second, more accessible theoretical analog, based on Ohm's law for electric current, to solve some of the same problems. Although not stated explicitly, the analog relies on Laplace's equation for the electric potential V [V] in a steady-state conductor, which results in direct correspondence between electric potential V and concentration C, electrical current I_{Elec} and diffusive transport I_{Diff}, and diffusivity D and conductivity σ. To illustrate the analogy between diffusive transport rate and electric current, we compared the simple, familiar examples of steady-state diffusion through a rectangular volume (Box 1, Figure 2a) and steady-state current in metal wire (Box 2, Figure 2b).

Table 2. Examples of transport processes governed by Laplace's equation.

	Transport process				
Feature	**Mass diffusion**	**Current flow**	**Heat conduction**	**Flow in porous media**	**Flow between parallel plates**
Flow law	Fick	Ohm	Fourier	Darcy	Pouiseuille
Potential	Concentration	Voltage	Temperature	Energy	Pressure
Conductance	Diffusivity	Conductivity	Thermal conductivity	Permeability/ viscosity	Separation^2/ viscosity
Zero-flux surface	Coated surface or mass-flow line	Insulated surface or current-flow line	Insulated surface or heat-flow line	Impermeable boundary or streamline	Impermeable boundary or streamline
Normal-flux surface	Equiconcentration surface	Equipotential surface	Isothermal surface	Equienergy surface	Equipressure surface
Continuity equation	∇ Mass flux = 0	∇ Current = 0	∇ Heat flux = 0	∇ Velocity = 0	∇ Velocity = 0
Laplace's equation	∇^2 Concentration = 0	∇^2 Voltage = 0	∇^2 Temperature = 0	∇^2 Energy = 0	∇^2 Energy = 0

Note: Adapted from Vaux (1961).

Box 1. Fick's laws of diffusion.

Macroscopic diffusion follows Fick's first law,

$$J_{\text{Diff}}[\text{mol m}^{-2}\,\text{s}^{-1}] = -D\frac{dC}{dx} \tag{1}$$

with solute flux due to diffusion J_{Diff} [mol s^{-1} m^{-2}] proportional to the spatial gradient, or derivative d/dx, of solute concentration C [mol m^{-3}]. The constant of proportionality is the diffusion coefficient D [m^2 s^{-1}], and the negative sign reflects that J_{Diff} is in the direction of lower concentration (down gradient) (Figure 1). The transport rate due to diffusion I_{Diff} [mol s^{-1}] is found by multiplying equation 1 by the cross-sectional area A [m^2],

$$I_{\text{Diff}}[\text{mol s}^{-1}] = -DA\frac{dC}{dx}\ . \tag{2}$$

Solute concentration C increases or decreases over time t [s], based on the conservation of mass (of solute),

$$\frac{dC}{dt}[\text{mol m}^{-3}\,\text{s}^{-1}] = \frac{dJ_{\text{Diff}}}{dx}\ .$$

With substitution from equation 1, $\frac{d}{dx}J_{\text{Diff}} = \frac{d}{dx}(-D\frac{dC}{dx})$, yielding Fick's second law:

$$\frac{dC}{dt}[\text{mol m}^{-3}\text{s}^{-1}] = -D\frac{d^2C}{dx^2}\ . \tag{3}$$

This result is satisfying intuitively: Over time, if the flux of solute into a parcel of length dx is smaller than the flux out, solute will accumulate. A key feature of equations 1 and 3, and of nature itself, is that J_{Diff} and dC/dt depend not on the magnitude of concentration but on the spatial gradient (Figure 1). At steady state, or equilibrium, solute neither accumulates nor declines (although molecules are still in constant motion), and

$$\frac{dC}{dt}[\text{mol m}^{-3}\text{s}^{-1}] = 0 = -D\frac{d^2C}{dx^2}\ .$$

If D is constant (not changing with C or x), then

$$\frac{dC}{dt}[\text{mol m}^{-3}\text{s}^{-1}] = 0 = \frac{d^2C}{dx^2}\ , \tag{4}$$

which is usually applicable for the dilute solutions of ecological interest (Cussler 1997).

A simple application of Fick's laws calculates diffusion through a rectangular volume in steady state, with constant concentrations at each end and concentration varying in only the x dimension (Figure 2a). The crucial question is the transport rate by diffusion I_{Diff} through the volume. It is answered by finding the solution of equation 4, or an expression for $C(x)$. Integrating both sides of equation 4 with respect to t gives

$$G_1[\text{mol m}^{-4}] = \frac{dC}{dx} + G_2\ ,$$

where G_1 and G_2 are constants of integration. Summing the constants into a third constant G [mol m^{-4}] gives $G = \frac{dC}{dx}$. Integrating both sides again, $Gx + H_1 = C + H_2$. Summing the constants H_1 and H_2 into H [mol m^{-3}] and solving for C provides the general solution

$$C(x)\ [\text{mol m}^{-3}] = Gx + H. \tag{5}$$

With the specified boundary conditions $C(x_0) = C_0$ and $C(x_L) = C_L$, the constants are determined by substitution in equation 5 to be $G = (C_L - C_0)/x_L$ and $H = C_0$ (the algebra being easier with H determined first). The exact solution is then

$$C(x)[\text{mol m}^{-3}] = \frac{(C_L - C_0)}{x_L}x + C_0 \tag{6}$$

(Figure 2a). The flux along the x-axis is obtained from Fick's first law, equation 1,

$$J_{\text{Diff}}[\text{mol m}^{-2}\,\text{s}^{-1}] = -D\tfrac{dC}{dx} = -D\frac{(C_L - C_0)}{x_L}\ , \tag{7}$$

and the quantity of typical interest, the transport I_{Diff}, is

$$I_{\text{Diff}}[\text{mol s}^{-1}] = -DA\frac{(C_L - C_0)}{x_L}\ . \tag{8}$$

This problem was described in one spatial dimension, x, but many real problems vary in three dimensions. In Cartesian coordinates, Fick's second law is

$$\frac{\partial C}{\partial t}[\text{mol m}^{-3}\,\text{s}^{-1}] = -D\left(\frac{\partial^2 C}{\partial x^2} + \frac{\partial^2 C}{\partial y^2} + \frac{\partial^2 C}{\partial z^2}\right) = -D\nabla^2 C\ , \tag{9}$$

where ∇^2 is the Laplacian operator[a]. At steady state in three dimensions,

$$\nabla^2 C[\text{mol m}^{-3}\text{s}^{-1}] = 0. \tag{10}$$

The result and notation in equation 10 hold true in any coordinate system. Equation 10, applied to functions other than C, is so familiar in physics that it has a name, Laplace's equation, and is indexed in many math and physics books.[b]

---

a. The symbol ∇, or del, is shorthand for the gradient "operator," which requires that the first partial derivative in space be applied to a function. The symbol ∇^2, or del squared, is shorthand for the Laplacian operator, which requires that the second partial derivative in three dimensions be applied. Other familiar operators include +, –, x, and $\int$. The Laplacian appears different among coordinate systems (Weisstein 2000), but the operation (second derivative) is the same.

b. Laplace's equation is also indexed under "Dirichlet problems" when boundary conditions are stated in terms of the function's value (e.g., C specified on a cell surface), and "Neumann problems" when boundary conditions are stated in terms of flux (e.g., J_{Diff} specified on a cell surface).

Box 2. Ohm's law.

For a typical metallic conductor such as wire, Ohm's law states that the electric current I_{Elec} is proportional to the electric potential difference V [V] measured along it, that is,

$$I_{Elec}[\mathrm{A}] = \frac{V}{R} ,$$

where the constant of proportionality is the resistance R [Ω]. Note that nonitalicized "A" represents the dimension Amperes (Table 1). Resistance is a property defined by an object's geometry and its resistivity ρ [Ω m], or conductivity σ [$1/\rho$; Ω^{-1} m^{-1}]. For a wire of length xL[m] and cross-sectional area A [m^2] (Figure 2b), $R = \sigma \frac{A}{x_L}$. The current is then

$$I_{Elec}[\mathrm{A}] = \sigma A \frac{(V_L - V_0)}{x_L} ,$$

similar to equation 8. Dividing by the area A gives the current density

$$J_{Elec}[\mathrm{A\ m^{-2}}] = \sigma \frac{(V_L - V_0)}{x_L} , \quad (11)$$

similar to equation 7. The formal equivalence between the linear functions in equations 7 and 11 implies that equations derived from one system hold true for the other, given consistent replacement of variables. Thus, in differential form,

$$J_{Elec}[\mathrm{A\ m^{-2}}] = \sigma \frac{dV}{dx} ,$$

as in equation 1. In three dimensions,

$$\frac{\partial V}{\partial t} = \sigma\left(\frac{\partial^2 V}{\partial x^2} + \frac{\partial^2 V}{\partial y^2} + \frac{\partial^2 V}{\partial z^2}\right) = \sigma \nabla^2 V ,$$

as in equation 9, and at steady state

$$\nabla^2 V[\mathrm{V\ m^{-3}s^{-1}}] = 0 ,$$

as in equation 10. Because circuits of general interest usually involve one-dimensional transport along wires, this equation is not common in texts, but it is appropriate for describing circuits involving three-dimensional electrolytic baths.

Note: See Halliday and Resnick (1978) for an alternate definition of Ohm's law. Ohm's law, like Fick's law, is not valid for materials that do not behave linearly. Non-Ohmian electrical conductors include semiconductors, in which the conductivity (and thus the current) does depend on the magnitude of the electric potential. Analogously, in non-Fickian materials, the diffusion coefficient (and thus flux) does change with concentration.

Model implementation

To implement the physical model, we created electric circuits of relevant geometries from conductive material immersed in electrolytic baths. Dimensions were scaled up to macroscopic proportions and nondimensionalized by reference to bacterial radii. Analogs for pore-fluid concentrations were made from disposable aluminum cookware (pie pans and baking sheets) and copper pipe, and analogs for bacteria were steel slingshot ammunition. They were all electrodes whose distributions of electric charges were uniform at each surface. Nonconductive boundaries were made from plastic tubs and plates, modeling clay, and adhesive shelf paper placed over aluminum surfaces. Electrolytic baths, made from sodium bicarbonate (chosen to reduce electrochemical plating on metal surfaces) dissolved in water (concentration adjusted to obtain appropriate current flow), constituted the resistance. Circuits were completed with 22-gauge, insulated copper wire using solder or alligator clips to steel (using stainless-steel soldering flux) and aluminum, respectively.

Circuits were driven with direct current (DC, via two D cell batteries) or alternating current (AC, via a signal generator limited to ~100 mA output). In the terminology of diffusion, the power source maintained constant "concentrations" at the boundaries by applying a constant voltage across the electrodes. These power supplies ensured the experimenters' safety and provided signals of sufficient magnitude and stability. Plating and bubble generation occurred but did not significantly influence the results. The DC power supply was simpler, but the AC power supply gave higher precision and reduced plating. Digital and analog multimeters were used to measure potential difference V [V] and current I [mA] in the circuits. All distances were measured to ±0.5 mm, and manipulations were made by hand.

Model validation

The physical model was tested against problems with known analytical solutions for the corresponding diffusion problems. We first tested the concentration–voltage analog by modeling steady-state diffusion from an outer cylinder to

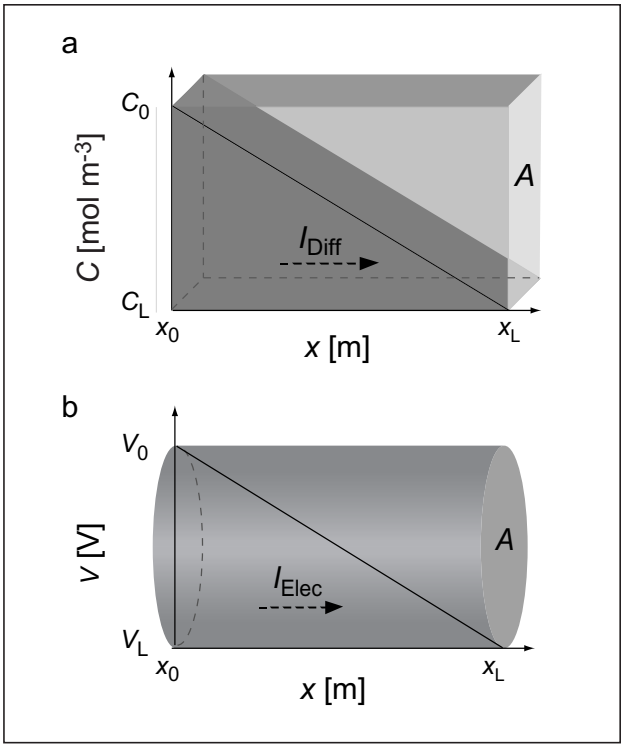

Figure 2. Schematic of diffusion–electric current analog (Boxes 1 and 2). (a) Steady-state diffusion through a rectangular volume of cross-sectional area A and length x_L, with constant concentrations C_0 and C_L at either end. (b) Steady-state current flow through a wire of cross-sectional area A and length x_L, with constant electric potential V_0 and V_L at either end.

an inner cylinder (Figure 3a; Crank 1975, eq. 5.2). The outer cylinder was made from a disposable aluminum cake pan (with vertical sides) with a 10 cm radius (r_{Out}). To insulate the bottom of the pan, adhesive shelf paper was glued to the bottom. To facilitate measurements, plain paper with printed radial coordinates was taped to the insulating paper. The inner cylinder was made from copper pipe, with a 1.0 cm external radius (r_{In}), taped to the bottom of the pan with double-sided foam tape. Because in this case diffusion is entirely radial, in cylindrical coordinates C varies only with radial distance r. Using a voltage probe oriented vertically and spanning the fluid depth (1 cm), we measured the electric potential averaged along the z axis for a given radius (r) and angle from the center point. We measured V along four orthogonal radii and averaged the values (Figure 3b).

The electric potential V increased from the surface of the inner cylinder outward along the radial axes. The electrical data matched closely the general analytical solution

$$C(r) = G + H \ln(r),$$

where G [mol m^{-3}] and H [mol m^{-3}] are constants dependent on boundary conditions. With the boundary conditions $C(r_{In}) = C_{In}$ and $C(r_{Out}) = C_{Out}$,

$$C(r) = \frac{C_{In} \ln\left(\frac{r_{Out}}{r}\right) + C_{Out} \ln\left(\frac{r}{r_{In}}\right)}{\ln\left(\frac{r_{Out}}{r_{In}}\right)},$$

In this problem, the modeled boundary conditions were $C_{In} = 0$ [mol m^{-3}] and $C_{Out} = 5.04$[mol m^{-3}], taken directly from the measured V_{In} and V_{Out}, respectively.

We then tested the relationship of real interest, that is, the current–diffusion analog, by using the geometry as described above while increasing the inner radius r_{In} from 0.1 to 6 cm. The inner cylinder was made from a strip of aluminum cut from a flat baking sheet, rolled into a cylinder, and secured with an alligator clip. At each step, the cylinder was unrolled, trimmed, and resecured. The experiment was completed twice (once each with AC and DC power). The current I_{Elec} was scaled to the maximum I_{Max} and the scaled values were averaged for the two experiments. The electrical data matched the analytical solution (from Crank 1975, eq. 5.5 divided by t) closely (Figure 3c):

$$I_{Diff}(r_{In}) = 2\pi D \frac{(C_{Out} - C_{In})}{(\ln(r_{Out}) - \ln(r_{In}))},$$

Given the boundary conditions and r_{Out} from above, we fit this equation to the data using the function Nonlinear Fit in Mathematica 4.1 (Wolfram Research), thereby estimating the parameter D. Note that in the cylindrical geometry here, diffusive transport I_{Diff} is not a linear function of the inner radius r_{In}, as it is in the spherical problem. These initial tests instilled confidence that we could use this easily implemented physical model of circuits on unsolved problems of steady-state diffusion. Though it is possible to use electrical analogs for time-dependent problems (Karplus and Soroka 1959), in-

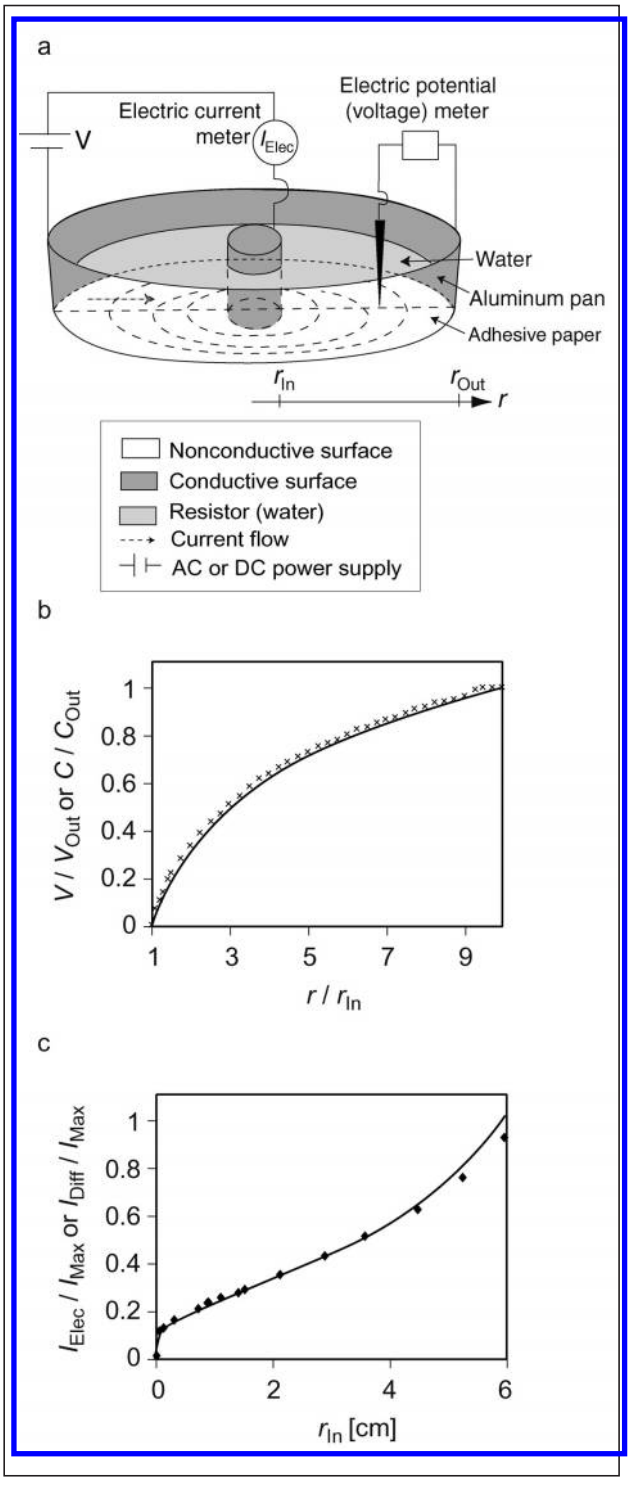

Figure 3. Model validation for the diffusion–electric current analog. (a) Schematic diagram of circuit used to solve problem of transport from an outer cylinder to an inner cylinder. (b) Concentration–electric potential analog. Line represents analytical solution and crosses represent electric potential measured along radial axis **r.** ***(c) Diffusive transport–electric current analog. Line represents analytical solution and diamonds represent electric current measured as the inner cylinder radius*** **r**$_{In}$ ***increased.***

vestment in apparatus and protocols may compare with that required for numerical modeling.

Diffusive flux to attached bacteria

We used the analog model to investigate how a surface-attached bacterium fares in obtaining nutrients by diffusive transport compared with a planktonic bacterium. The model mimicked a bacterium of radius r_B (here 0.5 cm) attached to an inert sediment-grain surface with a constant-concentration pore-fluid boundary parallel to the grain surface, at a fixed distance away from the bacterium (20 r_B; Figure 4a). The bacterium was assumed to be a perfect absorber, that is, $C = 0$ [mol m^{-3}] at the cell surface. With the bacterium and pore-fluid boundary fixed in place, the current I_{Elec} flowing through the circuit was measured as the insulating grain surface was moved a separation distance x_S [cm] away from the bacterium's outer surface (Figure 4a). We scaled the resulting current to that obtained without a grain surface present (I_{Elec}/I_{Free}, dimensionless) and scaled the separation distance to the bacterial radius (x_S/r_B, dimensionless). This problem is analogous to the heat-transfer problem of a buried heat sink abutted against an adiabatic surface, a problem that has not yet been solved analytically ("exactly") with consensus (Hahne and Grigull 1974, Small and Weihs 1977).

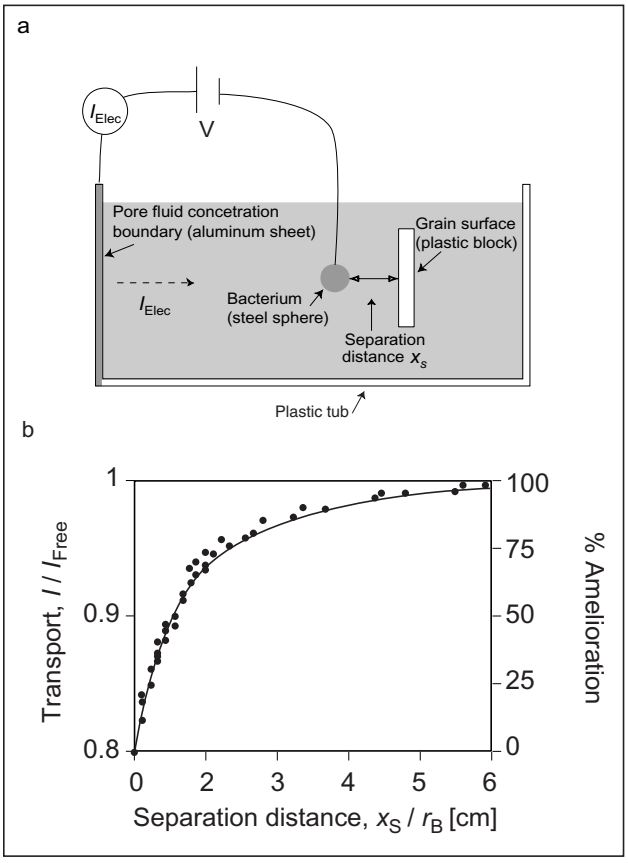

Figure 4. Effect of attachment on steady-state diffusive uptake by a spherical bacterium. (a) Cross-sectional schematic of electric circuit, where x_s is separation distance. (b) Influence of separation distance x_s on diffusive transport (I relative to that received by a freely suspended sphere, I_{Free}).

When the bacterium was tangential to the rigid surface, that is, $x_S = 0$, the current was about 80% of that of the unattached cell (Figure 4b). Thus, the cost of attachment in terms of lost access to diffusive transport was about 20% of the cell's potential gross uptake. In diffusionally constrained settings, the reason for attachment cannot be simple gain in nutrient acquisition. Rather, attached bacteria can be thought of as employing the feeding strategy of sessile marine invertebrates—that is, they let food come to them. When fluid advection (flow relative to the surface) is present, the diffusive sublayer over the grain surface will thin, thereby increasing nutrient supply as the same concentration difference is divided by a shorter distance. This complication illustrates the difficulty of comparing two distinct foraging strategies over ecological and evolutionary time scales. Who wins? The attached bacterium isolated in the diffusive sublayer, which may be thinned by flow, or the motile suspended bacterium that can spend more time in high-concentration fluid (Mitchell et al. 1996, Dusenbery 1999, Konopka 2000)? In porous environments with significant advection and periodic sediment suspension, attachment may be the only way to exploit the habitat over long time periods.

Attachment cost dropped to about 5% when the bacterium was one cell diameter away from the grain surface (Figure 4b). The rapid amelioration of uptake cost with increasing separation suggests that attached bacteria capable of maintaining a distance of at least one radius away from a solid surface would have a distinct advantage over those abutted directly to the surface. This result immediately prompts speculation about the role of extracellular material in microbial ecology. Extracellular polysaccharide (EPS) is often produced in large volume by attached bacteria in plush and sparse biofilms (Figure 5; Underwood et al. 1995, Heissenberger et al. 1996, Bennett et al. 1999, Ransom et al. 1999). As a first approximation, EPS and water have identical transport properties for the diffusion of small molecules, that is, Ds for small molecules in the two media are not substantially different (Koch 1990, Cussler 1997). These results suggest that EPS may act in part to hold cells a fixed distance from a surface in order to improve diffusive transport of nutrients.

Sediment-grain topography

Uncovering relationships between foraging and habitat relies on characterizing spatial effects at the organism's scale. For example, sediment grains display a wide range of microtopography, typically expressed in bulk as the surface area per unit of volume. Rounded sand grains are often modeled as Euclidean surfaces, but silt and clay grains can contain up to two orders of magnitude more surface area per unit of volume because of a higher surface-to-volume ratio and increased surface relief. On a given grain, bacterial attachment can occur at topographic highs (bumps) or lows (pits) (Figure 6a). Attachment at a topographic low might provide refuge from

grazing (DeFlaun and Mayer 1983), but this benefit could involve a substantial tradeoff in terms of nutrient flux.

Using the same setup as before, with a malleable, nonconductive surface (modeling clay), we investigated the effects of sediment features, such as pits and bumps, on diffusive flux. We changed the grain topography (feature radius r/r_B and relief x_H/r_B) and measured the resulting current I_{Elec} passing through the circuit (Figure 6b). The current, scaled to that received by the cell on a flat surface (I_{Elec}/I_{Flat}, dimensionless), increased slightly for the bacterium on bumps and decreased severely for the bacterium in pits (Figure 6c). The uptake varied sixfold over the range of topography examined. Thus, deep, narrow pits may be excellent places to survive predation, but they are not good foraging locations. DeFlaun and Mayer (1983) noted a lack of bacteria in bacteria-sized pits on sediment grains. For attachment in bacterium-sized pits ($x_H/r_B = 2$ and $r/r_B = 1$), the modeled uptake of limiting nutrient was reduced by about 50% (Figure 6c).

Multiple cells and clonal fitness

Because cell signaling by bacteria can involve coordinated and perhaps cooperative behavior, bacteria have been suggested to function like modular (Andrews 1998) or multicellular (Shapiro 1998) organisms and to evolve at multiple levels of

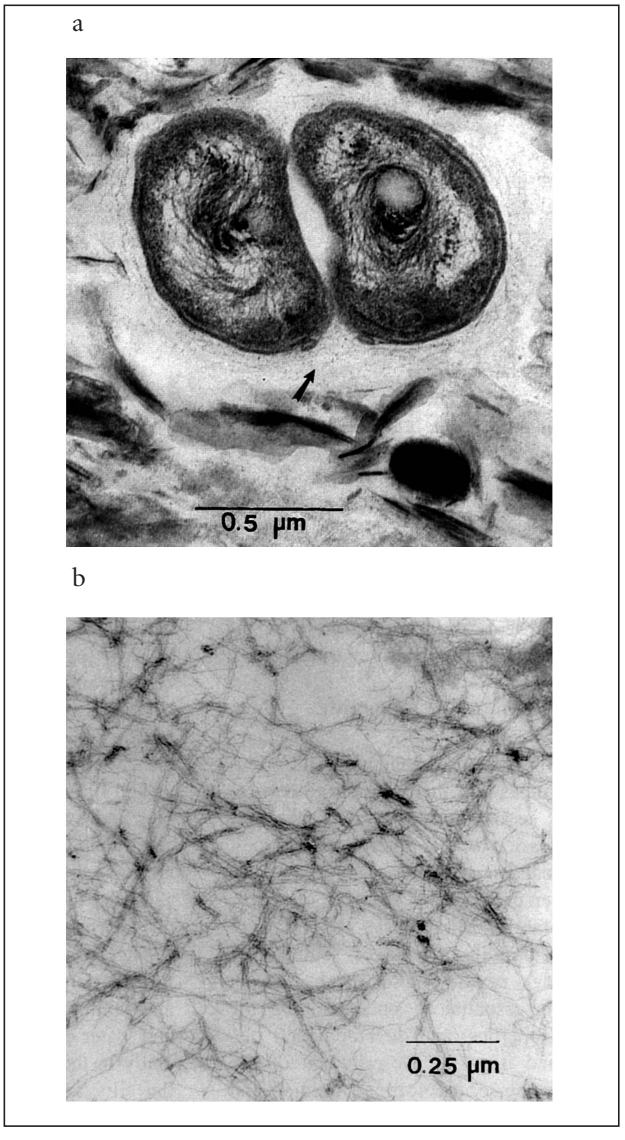

Figure 5. Extracellular polysaccharides (EPSs) associated with bacteria in sediments as identified with transmission electron microscopy. (a) High volume of EPS surrounding two dividing cells showing their distance from the surrounding grains. (b) Higher magnification view showing gel matrix of EPS with open pore spaces. Reprinted from Bennett et al. (1999), with permission from Elsevier Science.

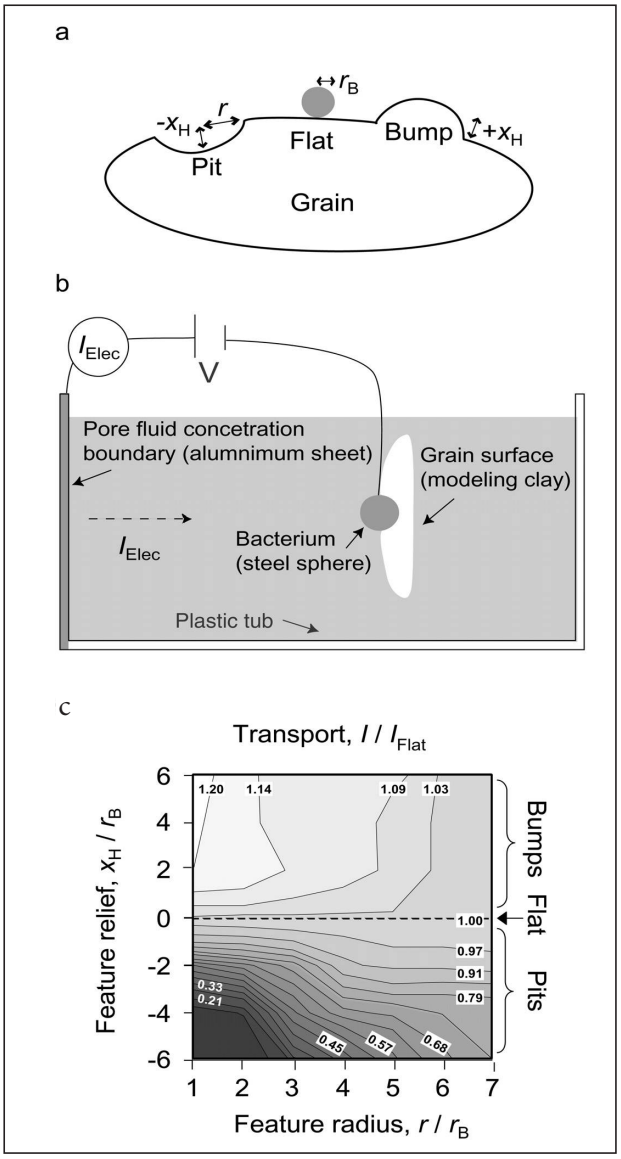

Figure 6. Influence of local sediment-grain topography on steady-state uptake by attached bacteria. (a) Geometry used to define topographic pits and bumps. (b) Schematic configuration of electric circuit. (c) Contour plot of transport to the bacterium depending on surface relief. Lines represent transport relative to that obtained by a cell on a flat surface, I_{Flat}.

selection (Caldwell et al. 1997). As in the ecology of higher organisms, however, observing cooperative behavior is insufficient to establish higher-order (kin) selection. Studies of marmot warning calls illustrate the arduous task of quantifying the fitness costs and gains and the "genetic relatedness" that is required to posit the evolution of a cooperative behavior (Blumstein and Armitage 1998, Hauber and Sherman 1998).

We conjecture that in a small volume of sedimentary habitat (10–100 μm^3), most of the bacteria of a particular species may be members of the same clone, having nearly 100% of their DNA in common and thus genetic relatedness close to 1. As an initial step in understanding whether typical benthic bacteria have evolved under clonal selection (as the first level of higher-order selection), we sought to develop predictive theory for clonal foraging by surface-attached bacteria.

We began with a theory based on individual fitness (reproductive success by the succeeding generation), using solute uptake as a proxy for energy gain. Because of differing metabolic costs tied to foraging strategies, the gross nutrient uptake rate is insufficient to predict fitness. Rather, the net nutrient uptake rate is often suggested to correlate with individual fitness F_{Ind}. As above, we assumed that all solute transport was due to diffusion and that uptake equaled diffusive transport I_{Ind} to the individual cell surface, that is, the cells were perfect absorbers. Thus, individual fitness F_{Ind}[mol s^{-1}] was the net rate of gain

$$F_{Ind}\,[\text{mol s}^{-1}] = I_{Ind} - M_{Ind},$$

where M_{Ind}[mol s^{-1}] is the metabolic cost of maintaining the organism.

We then defined clonal fitness F_{Clone} [mol s^{-1}] as the net uptake rate of all the bacteria belonging to the clone

$$F_{Clone}\,[\text{mol s}^{-1}] = I_{Clone} - M_{Clone},$$

where the metabolic gains and costs equaled the sums of the individual rates. In this equation, I_{Clone} is the clonal uptake, and M_{Clone} is the metabolic cost of maintaining the clone. As a first approximation, we assumed uniform basal metabolic costs among the clone members, such that

$$F_{Clone}\,[\text{mol s}^{-1}] = I_{Clone} - N_B\,M_{Ind},$$

where N_B is the number of bacteria in the clone.

The uptake, or transport I_{Clone}, is not a simple linear function of cell number because of competition for nutrients among neighbors. To solve this problem, we followed the arguments that Berg and Purcell (1977) and Berg (1993) developed to model the uptake by multiple receptors on a single cell, based on the analog of "diffusive resistors" in parallel (Figure 7a, 7b). As a first step, we followed their approach theoretically to calculate the clonal uptake I_{Clone} by disk-shaped bacteria attached to sediment grain of radius r_G (with the origin at the center of the grain). The dissolved limiting nutrient was assumed to be at a constant concentration at $r = \infty$ (Figure 7a). In fact, staring at Berg's (1993) cartoon of multiple receptors on a cell, after peering at bacteria on sand grains under a microscope, stimulated this research. Following Berg (1993), while scaling the number of bacteria N_B to the maximum possible for a complete monolayer of bacteria,

$$\frac{I_{Clone}}{I_{Full}} = \frac{1}{1+\frac{\pi}{4}\frac{N_{Full}}{N_B}\frac{r_B}{r_G}}.$$

The number of bacteria N_{Full} for a complete monolayer coverage of the grain was calculated as the grain surface area ($4\pi r_G^2$) divided by the area per bacterium (πr_B^2), without correcting for the empty space between projected circles (an error of 10% at most) (Weisstein 2000, "Circle Packing").

Berg and Purcell (1977) and Berg (1993) showed that a very small number of receptors is needed on a cell's surface before it receives nearly all that it would have by having the entire surface covered with receptors. For geometry representative of bacteria on a sand grain ($r_G/r_B = 100$), scant coverage of the surface was needed before I_{Clone}/I_{Full} reached 0.90, or 90% of what it would get if the entire grain surface were covered by bacteria (Figure 7c). This function, similar in form to the Michaelis-Menten equation for saturating enzyme kinetics, increased steeply and leveled off to approach $I_{Clone}/I_{Full} = 1$ asymptotically as the fraction of surface area covered by bacteria increased. We improved our physical intuition for the problem by employing physical models that included adhesive paper, with holes punched out, attached to aluminum surfaces.

To improve the realism of the theoretical model, we predicted clonal uptake by spherical bacteria with the constant-concentration boundary at a finite, rather than infinite, distance x_F away. We interpreted the characteristic length x_F as half the distance to a neighboring sediment grain, where in a symmetrical pore (space between grains) lined by absorbing bacteria, the concentration would be highest. We modeled the bacteria attached to a flat plate in order to simplify the mathematics and because the curvature of a large grain should not be influential at the bacterium's scale. The "diffusive resistance" of each bacterium was estimated using the "shape factor" put forth by Hahne and Grigull (1974), resulting in an effective radius equal to ~$2r_B$. Uptake was then calculated as

$$\frac{I_{Clone}}{I_{Full}} = \frac{Ax_F\frac{N_B}{N_{Full}}}{2\pi r_B^2\left(1+2x_F\frac{N_B}{N_{Full}}\right)},$$

where A is the area of the surface. Uptake increased more rapidly, compared with disk-shaped bacteria, as the fraction of surface covered by bacteria increased (Figure 7d). It is also worth noting that, unlike coverage by transport sites in a cell membrane, it is possible to have more than 100% coverage of the grain surface by bacteria by stacking them in various arrangements more than a single bacterium thick. We did not go to these lengths because of the obviously diminishing nutrient returns at well short of what we termed 100% coverage.

We calculated clonal fitness based on idealized metabolic costs (low, medium, and high) (Figure 7d, 7e). Thus, whereas costs increased linearly as clone mates were added (near-neighbor progeny produced), gross uptake approached an asymptote, and the difference, or clonal fitness F_{Clone}, reached a maximum at well below 100% coverage. The higher the

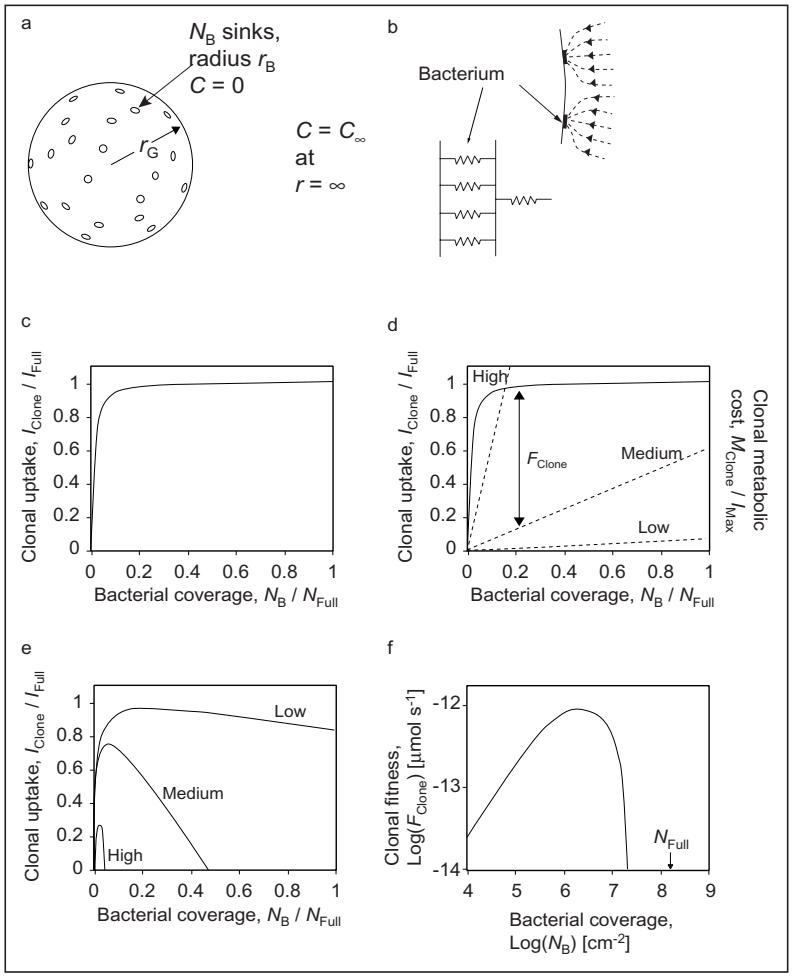

Figure 7. Modeled clonal foraging and fitness. (a) Schematic of uptake by clonal bacteria attached to sediment grain bathed in fluid. Taken from Berg (1993), as developed for uptake by multiple receptors on a single cell, with symbols modified to mirror this text (reprinted by permission of Princeton University Press). (b) Schematic of electrical analogy, where the "diffusive resistance" of each absorber is obtained and then analyzed as for resistors in parallel. (c) Model results of diffusive uptake by a (clonal) population of disk-shaped bacteria on a spherical grain, as a function of the fraction of grain surface covered by bacteria, with uptake scaled to the uptake calculated for population covering the surface with a monolayer of cells (I_{Full}). Only a small fraction of the surface needed to be covered by bacteria (N_B/N_{Full}) before the clone received nearly all that it would by covering the surface completely. Note that with a constant solute concentration at r_∞, uptake I_{Clone}/I_{Full} depends also on the parameter r_G/r_B (here equal to 100). (d) Model results of diffusive uptake by a (clonal) population of spherical bacteria attached to a flat plate, showing that uptake increased rapidly with increasing coverage by bacteria. Dashed lines represent idealized metabolic costs to the population, which increase linearly with population size. Successive differences among low, medium, and high costs were 10-fold. Arrow represents graphically the calculation of clonal fitness as the difference between population gains and costs. (e) Clonal fitness given idealized costs and gains in (d). For high ratios of cost to nutrient supply (uptake), clonal fitness shows pronounced optima with scant bacterial coverage of the surface. (f) Clonal fitness given values attainable in nutrient-poor sands: $r_B = 0.5$ µm, $x_F = 50$ µm, $C_F = 5$ µM (limiting nutrient of C), $M_{Ind} = 5 \times 10{-}14$ µm s^{-1} (based on 1 × 10–14 g C $cell^{-1}$, growth efficiency = 10%, and doubling time of 2 days), and $D = 1 \mu 10^{-5}$ cm^2 s^{-1}.

metabolic costs (relative to a fixed nutrient supply), the more pronounced were the optima in coverage. In Berg's (1993) analysis of the receptors on a single cell, he stated that the paucity of coverage required to approach I_{Full} leaves room for all of the different receptor types that a cell needs. This analogy should extend to microbial consortia on grain surfaces, where there would be room for multiple types of cells involved in the breakdown of complex substrates, as suggested by Koch (1990).

Depending on the metabolic cost-to-nutrient-supply ratio, a clone may decrease its fitness by producing near neighbors. Reduced fitness for high-density clones was predicted with parameter values attainable in surficial sands (Figure 7f). In such cases, attached bacteria may be predicted to produce motile progeny rather than near neighbors. Though greatly simplified, this type of modeling allows development of quantitative predictions for conditions favoring allocation of resources to dispersal (Caldwell and Lawrence 1986, Lawrence and Caldwell 1988).

For a given strain, cell size, cost per cell, and bulk solute concentration, one way that the nutrient supply changes in nature is by advective thinning of the diffusive boundary layer over a surface. This method gives a way to predict quantitatively how thinning of the boundary layer over a grain surface should result in denser bacterial populations. Laboratory experiments could be used to test the hypothesis that clonal bacterial foraging is explained better by maximizing clonal rather than individual fitness. Implicit in the hypothesized density-dependent foraging strategy is inclusion of quorum sensing. We emphasize that quorum sensing is the use of signals to determine a combination of population density (signal accumulation) *and* hydrodynamic conditions (signal depletion). We also note that the modeling described here, both theoretical and analytical, could be adapted to investigate bacteria as sources, rather than sinks, of solute molecules. Brookfield (1998) showed theoretically how quorum sensing may be a stable strategy under certain conditions. In an experiment tracing the evolution of *Myxococcus xanthus* over 1,000 generations, Velicer and colleagues (1998) found that the evolution of social behaviors, coordinated by chemical signaling, depended on the hydrodynamics of the habitat.

Summary

We implemented an electric-circuit analog to the diffusive process, which was successful for examining issues of nutrient uptake by attached bacteria. We used the formal equivalence of Ohm's and Fick's laws to provide quantitative solutions to mi-

crobial foraging questions that have been intractable with analytical and introductory numerical techniques. The technique is applicable to any system governed by Laplace's equation, which describes many forms of mass or energy transfer at steady state. The technique is easy and inexpensive. Furthermore, the solutions are real and exact and do not rely on definable gridding or boundary conditions.

The benefits of this physical model are many. It rapidly approaches steady state (instantaneous to the observer) and provides real-time feedback during manipulations. For microbiologists, it builds intuition of organism-scale processes while working at a macroscopic scale. Boundary conditions are physical rather than symbolic (as in analytical models) or digital (as in numerical models) and so can be grasped both literally and visually. The method could easily be adapted, for example, to investigate uptake by single cells with complex shapes (such as diatoms and dinoflagellates), complex geometries of diagenetic reactions, and diffusion-like transport of populations through complex habitat. The electrical model can also be used in the implementation of curricula apt for "hands- and minds-on" learning (Lynch 1997, Moreno 1999). Many engineering texts on transport processes (Karplus and Soroka 1959, Welty et al. 1984) contain brief discussions of experimental methods for two-dimensional experiments, using carbon paper and silver paint to create desired geometries.

Using the electrical analog, we found that a cell attached to a flat surface loses about 20% of its potential uptake. This cost all but vanishes when the bacterium is maintained at a single bacterial diameter away from the surface, generating the hypothesis that one role of bacterial EPS is to maintain a fixed distance from the surface. Conversely, protection in a bacterium-sized pit comes at a cost of 50% of an attached cell's potential nutrient uptake.

When multiple bacteria were attached to a planar surface, the combined diffusion current increased steeply with the percentage of surface covered by bacteria and reached 90% of that possible with 100% coverage with less than 2% of the surface occupied. We calculated that, depending on specific metabolic costs, the combined net gain of multiple cells can be maximal at well below 100% coverage. In benthic systems, approximately 0.1%–2% of sediment-grain surfaces are covered by bacteria; a clonal population using a dissolved resource therefore might better partition growth to progeny that disperse (i.e., motile cells) than to producing near neighbors.

Acknowledgments

The authors wish to thank Peter Rhines, David Dusenbery, Daniel Grubaum, and the participants in Friday Harbor Lab's 1999 Marine Chemosensory Ecology Course for productive discussions; Fritz Star, Christian Sarason Parker, and Christopher Krembs for critical reviews of earlier drafts; and Eric Lindahl, Michael O'Donnell, and Rex Johnson for help with the model implementation. This work was conducted with support from the Office of Naval Research and Friday Harbor Labs, University of Washington.

References cited

Andrews JH. 1998. Bacteria as modular organisms. Annual Review of Microbiology 52: 105–126.

Bachofen R, Schenk A. 1998. Quorum sensing autoinducers: Do they play a role in natural microbial habitats? Microbiological Research 153: 61–63.

Ben-Ari ET. 1999. Not just slime—beneath the slippery exterior of a microbial biofilm lies a remarkably organized community of organisms. BioScience 49: 689–695.

Bennett RH, Ransom B, Kastner M, Baerwald RJ, Hulbert MH, Sawyer WB, Olsen H, Lambert MW. 1999. Early diagenesis: Impact of organic matter on mass physical properties and processes, California continental margin. Marine Geology 159: 7–34.

Berg HC. 1993. Random Walks in Biology. Rev. ed. Princeton (NJ): Princeton University Press.

Berg HC, Purcell EM. 1977. The physics of chemoreception. Biophysics 20: 193–219.

Blumstein DT, Armitage KB. 1998. Why do yellow-bellied marmots call? Animal Behaviour 56: 1053–1055.

Brookfield JFY. 1998. Quorum sensing and group selection. Evolution 52: 1263–1269.

Caldwell DE, Lawrence JR. 1986. Growth kinetics of *Pseudomonas fluorescens* microcolonies within the hydrodynamic boundary layers of surface microenvironments. Microbial Ecology 12: 299–312.

Caldwell DE, Wolfaardt GM, Korber DR, Lawrence JR. 1997. Do bacterial communities transcend Darwinism? Advances in Microbial Ecology 15: 105–191.

Carslaw HS, Jaeger JC. 1959. Conduction of Heat in Solids. Oxford (UK): Clarendon Press.

Chernin LS, Winson MK, Thompson JM, Haran S, Bycroft BW, Chet I, Williams P, Stewart GSAB. 1998. Chitinolytic activity in *Chromobacterium violaceum:* Substrate analysis and regulation by quorum sensing. Journal of Bacteriology 180: 4435–4441.

Costerton JW. 1995. Overview of microbial biofilms. Journal of Industrial Microbiology 15: 137–140.

Crank J. 1975. The Mathematics of Diffusion. Oxford (UK): Oxford University Press.

Cussler EL. 1997. Diffusion: Mass Transfer in Fluid Systems. New York: Cambridge University Press.

DeFlaun MF, Mayer LM. 1983. Relationships between bacteria and grain surfaces in intertidal sediments. Limnology and Oceanography 28: 873–881.

Dugatkin LA. 1997. The evolution of cooperation. BioScience 47: 355–362.

Dusenbery DB. 1999. Fitness landscapes for effects of shape on chemotaxis and other behaviors of bacteria. Journal of Bacteriology 180: 5978–5983.

Fuqua WC, Winans SC, Greenberg EP. 1994. Quorum sensing in bacteria: The LuxR-LuxI family of cell density-responsive transcriptional regulators. Journal of Bacteriology 176: 269–275.

———. 1996. Census and consensus in bacterial ecosystems: The LuxR-LuxI family of quorum-sensing transcriptional regulators. Annual Review of Microbiology 50: 727–751.

Gebhart B. 1993. Heat Conduction and Mass Diffusion. New York: McGraw-Hill.

Givskov M, Eberl L, Molin S. 1997. Control of exoenzyme production, motility and cell differentiation in *Serratia liquefaciens.* FEMS Microbiology Letters 148: 115–122.

Hahne E, Grigull U. 1974. A shape factor scheme for point source configurations. International Journal of Heat and Mass Transfer 17: 267–273.

Halliday D, Resnick R. 1978. Physics: Part II. New York: John Wiley and Sons.

Hauber ME, Sherman PW. 1998. Nepotism and marmot alarm calling. Animal Behaviour 56: 1049–1052.

Heissenberger A, Leppard GG, Herndl GJ. 1996. Ultrastructure of marine snow, II. Microbiological considerations. Marine Ecology Progress Series 135: 299–308.

Johnson AT. 1999. Biological Process Engineering: An Analogical Approach to Fluid Flow, Heat Transfer, and Mass Transfer Applied to Biological Systems. New York: John Wiley and Sons.

Kaiser D, Losick R. 1997. Why and how bacteria communicate. Scientific American 276: 68–73.

Karp-Boss L, Boss E, Jumars PA. 1996. Nutrient fluxes to planktonic osmotrophs in the presence of fluid motion. Oceanography and Marine Biology: An Annual Review 34: 71–107.

Karplus WJ, Soroka WW. 1959. Analog Methods: Computation and Simulation. New York: McGraw-Hill.

Kaye BH. 1989. A Random Walk through Fractional Dimensions. Weinheim (Germany): VCH Publishing.

Koch AL. 1990. Diffusion: The crucial process in many aspects of the biology of bacteria. Advances in Microbial Ecology 11: 37–71.

Koch AL, Wang CH. 1982. How close to the theoretical diffusion limit do bacterial uptake systems function? Archives of Microbiology 131: 36–42.

Konopka A. 2000. Theoretical analysis of the starvation response under substrate pulses. Microbial Ecology 38: 321–329.

Lawrence JR, Caldwell DE. 1988. Behavior of bacterial stream populations within the hydrodynamic boundary layers of surface microenvironments. Microbial Ecology 4: 15–27.

Lynch S. 1997. Novice teachers' encounter with national science education reform: Entanglements or intelligent interconnections? Journal of Research in Science Teaching 34: 3–17.

McLean RJC, Whiteley M, Stickler DJ, Fuqua WC. 1997. Evidence of autoinducer activity in naturally occurring biofilms. Fems Microbiology Letters 154: 259–263.

Mitchell JG, Pearson L, Dillon S. 1996. Clustering of marine bacteria in seawater enrichments. Applied and Environmental Microbiology 62: 3716–3721.

Moreno NP. 1999. K–12 science education reform—a primer for scientists. BioScience 49: 569–576.

Narasimhan TN. 1999. Fourier's heat conduction equation: History, influence, and connections. Reviews of Geophysics 37: 151–172.

Pace NR. 1997. A molecular view of microbial diversity and the biosphere. Science 2276: 734-740.

Paerl HW, Pinckney JL. 1996. A mini-review of microbial consortia: Their roles in aquatic production and biogeochemical cycling. Microbial Ecology 31: 225–247.

Pasciak WJ, Gavis J. 1974. Transport limitation of nutrient uptake in phytoplankton. Limnology and Oceanography 19: 881–888.

Ploug H, Stolte W, Jorgensen BB. 1999. Diffusive boundary layers of the colony-forming plankton alga *Phaeocystis* sp.—Implications for nutrient uptake and cellular growth. Limnology and Oceanography 44: 1959–1967.

Ransom B, Bennett RH, Baerwald R, Hulbert VH, Burkett PJ. 1999. *In situ* conditions and interactions between microbes and minerals in fine-grained marine sediments: A TEM microfabric perspective. American Mineralogist 84: 183–192.

Rutherford J, Ahlgren A. 1989. Science for All Americans. New York: Oxford University Press.

Segall JE, Ishihara A, Berg HD. 1985. Chemotactic signaling in filamentous cells of *Escherichia coli.* Journal of Bacteriology 161: 51–59.

Shapiro JA. 1998. Thinking about bacterial populations as multicellular organisms. Annual Review of Microbiology 52: 81–104.

Small RD, Weihs D. 1977. Thermal traces of a buried heat source. ASME Journal of Heat Transfer 99: 47–53.

Srinivasan S, Ostling J, Charlton T, de Nys R, Takayama K, Kjelleberg S. 1998. Extracellular signal molecule(s) involved in the carbon starvation response of marine *Vibrio* sp. strain S14. Journal of Bacteriology 180: 201–209.

Steward GF, Smith DC, Azam F. 1996. Abundance and production of bacteria and viruses in the Bering and Chukchi Seas. Marine Ecology Progess Series 131: 287–300.

Tunlid A. 1999. Molecular biology: A linkage between microbial ecology, general ecology and organismal biology. Oikos 85: 177–189.

Underwood GJC, Paterson DM, Parkes RJ. 1995. The measurement of microbial carbohydrate exopolymers from intertidal sediments. Limnology and Oceanography 40: 1243–1253.

Vaux WG. 1961. Fluid flow in the open-surfaced porous bed. Master's thesis. University of Minnesota, Minneapolis.

Velicer GJ, Kroos L, Lenski RE. 1998. Loss of social behaviors by *Myxococcus xanthus* during evolution in an unstructured habitat. Proceedings of the National Academy of Sciences 95: 12376–12380.

Vetter YA, Deming JW, Jumars PA. 1998. A predictive model of bacterial foraging by means of freely-released extracellular enzymes. Microbial Ecology 36: 75–92.

Weisstein E. 2000. Eric Weisstein's World of Mathematics. (26 Jan. 2002; *www.mathworld.wolfram.com*)

Welty JR, Wicks CE, Wilson RE. 1984. Fundamentals of momentum, heat and mass transfer. 3rd ed. New York: John Wiley and Sons.

Wilson T, Hastings J. 1998. Bioluminescence. Annual Review of Cell and Developmental Biology 14: 197–230.

Wolfaardt GM, Lawrence JR, Roberts RD, Caldwell DE. 1994. The role of interactions, sessile growth and nutrient amendments on the degradative efficiency of a microbial consortium. Canadian Journal of Microbiology 40: 331–340.